Smart inverse design of graphene-based photonic metamaterials by an adaptive artificial neural network

Article *in* Nanoscale · May 2019

DOI: 10.1039/C9NR01315F

CITATIONS
6

READS
181

5 authors, including:

Yingshi Chen
Xiamen University
5 PUBLICATIONS **9** CITATIONS

SEE PROFILE

Jinfeng Zhu
Xiamen University
68 PUBLICATIONS **1,014** CITATIONS

SEE PROFILE

Nanoscale

Accepted Manuscript

This article can be cited before page numbers have been issued, to do this please use: Y. Chen, J. Zhu, Y. Xie, N. Feng and Q. H. H. Liu, *Nanoscale*, 2019, DOI: 10.1039/C9NR01315F.

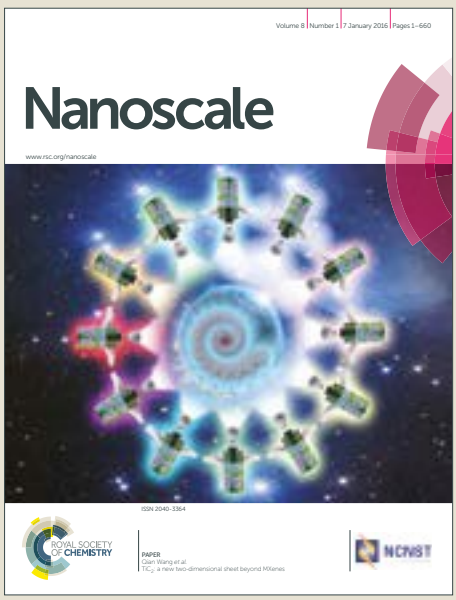

ROYAL SOCIETY OF CHEMISTRY

rsc.li/nanoscale

View Article Online
DOI: 10.1039/C9NR01315F

Nanoscale

ARTICLE

Smart inverse design of graphene-based photonic metamaterials by an adaptive artificial neural network

Yingshi Chen,[a] Jinfeng Zhu,*[a] Yinong Xie,[a] Naixing Feng[b] and Qing Huo Liu*[c]

Received 00th January 20xx,
Accepted 00th January 20xx

DOI: 10.1039/x0xx00000x

www.rsc.org/

The burgeoning research of graphene and other 2D materials enables many unprecedented metamaterials and metadevices for applications on nanophotonics. The design of on-demand graphene-based metamaterials often calls for the solution of a complex inverse problem within a small sampling space, which highly depends on the rich experiences from researchers of nanophotonics. Conventional optimization algorithms could be used for this inverse design, but they converge to local optimal solutions and take significant computational costs with increased nanostructure parameters. Here, we establish a deep learning method based on an adaptive batch-normalized neural network, aiming to implement smart and rapid inverse design for graphene-based metamaterials with on-demand optical responses. This method allows a quick converging speed with high precision and low computational consumption. As typical complex proof-of-concept examples, the optical metamaterials consisting of graphene/dielectric alternating multilayers are chosen to demonstrate the validity of our design paradigm. Our method demonstrates a high prediction accuracy of over 95% after very few training epochs. A universal programming package is developed to achieve the design goals of graphene-based metamaterials with low absorption and near unity absorption, respectively. Our work may find important design applications in the field of nanoscale photonics based on graphene and other 2D materials.

Introduction

The rise of graphene and other 2D materials has brought about many new opportunities for the novel optical design of metamaterials and metadevices, and boosted the development of advanced optics from nano-optics to angstrom-optics [1-4]. Due to the exceptional electrical and optical properties of 2D materials, their metamaterials with extraordinary performance can be developed in many fields of optics, including photodetection, photovoltaics, electro-optic modulation, optical sensing and light absorption [5-9]. The design of photonic metamaterials using 2D materials relies on various application requirements, and implicates solving complex inverse problems by numerous electromagnetic simulations, which usually requires rich experiences and dedicated efforts from experts in optical engineering [10-12]. This is usually time-consuming and limited by a small library of known optical structures and devices for the optics of 2D materials. In order to mitigate such a barrier, some conventional optimization algorithms may be adopted, such as genetic algorithm, particle swarm, convex optimization, topology optimization and variational Born iterative method [13-17]. Nevertheless, these algorithms often converge to the local optimal solutions, and take significant computational costs with increased multiple nanostructure parameters. Therefore, a more efficient scheme is still in demand for the metamaterial design based on 2D materials [18].

Very recently, the algorithm of deep learning has shown promising potential in solving inverse design problems of nanophotonics with higher efficiency and accuracy. On-demand design by deep learning has been used in many conventional structures of nanophotonics, such as multilayer nanoparticles, multilayer films, metamaterials, metasurfaces, plasmonic nanostructures [19-23]. Compared with the wide applications of deep learning in video and audio recognition, the sampling space for the design of nanophotonics is relatively smaller with a limited number of samples. Up to now, despite the significance of 2D materials in advanced optics, the use of deep learning for their metamaterial design is barely reported.

On the other hand, the up-to-date technique of batch normalization (BN) is a milestone in the development of deep learning [24], which has sped up the convergence rate of many neural networks and achieved higher prediction accuracy for many scientific and engineering inverse problems, but it is still not applied in the inverse design of nanophotonics. This technique uses the additional BN layers in the conventional artificial neural network, in order to obtain some statistics features for each batch. Although these features might have a certain degree of errors, classical deep learning paradigms (such as the recognition of images, videos and audios) could adopt a huge sampling space to average these errors and approach a feasible descent direction. Nevertheless, in many cases with

[a] School of Electronic Science and Engineering, Xiamen University, Xiamen 361005, China. E-mail: nanoantenna@hotmail.com
[b] College of Electronic Science and Technology, Shenzhen University, Shenzhen 518060, China
[c] Department of Electrical and Computer Engineering, Duke University, Durham, North Carolina 27708, USA. E-mail: qhliu@duke.edu
Electronic Supplementary Information (ESI) available: [details of any supplementary information available should be included here]. See DOI: 10.1039/x0xx00000x

View Article Online
DOI: 10.1039/C9NR01315F

small sampling spaces, such as the inverse design of nanophotonics, the errors would lead to wrong calculation directions. In many circumstances, the predicted results might be even worse than those obtained by the conventional artificial neural network. Thus, the error criterion of BN might increase for the small sampling space in the design of nanophotonics with an inadequate batch statistics estimation, which would hinder the usage of BN in this field. Due to this fact, the sophisticated BN approach of deep learning has not been adopted in the previous reports for the structure design of nanophotonics. For this reason, an improved method with BN that can find and learn more features from a small sampling space is quite in demand, in order to solve the design problems of nanophotonics.

Here, we propose a simple yet effective algorithm, called adaptive BN, which improve both the convergence rate and the prediction accuracy for the inverse optical design of metamaterials based on graphene. In our approach, the on-demand spectrum is input and processed by an adaptive normalized neural network, in order to output the corresponding metamaterial based on 2D materials. As typical complex proof-of-concept examples, the inverse optical design for graphene/Si_3N_4 multilayer metamaterial is evaluated, and shows higher computational efficiency and better prediction consistency with the on-demand spectrum, compared with conventional deep-learning algorithms. Our method implies the strong capability in quickly predicting the complex optical properties of metamaterials and metadevices based on graphene and other 2D materials.

Methodology

In order to demonstrate the capability of the designated deep learning method, we use a specific example of graphene to illustrate the complexity in training deep neural network of inverse optical design for metamaterials based on 2D materials. As shown in Fig. 1, we investigate a thin film metamaterial consisting of alternating layers of graphene and Si_3N_4, and the excitation light is introduced through a hemispheric prism with an incident angle θ and a certain polarization (*e.g. s*- or *p*-polarizations). The purpose of the inverse optical design for this multilayer film is to generate a target absorbance spectrum (e.g. perfect light absorption at a certain central wavelength), and the design space is the thickness of each Si_3N_4 layer. The multilayer structure has m alternating layers of graphene and Si_3N_4 with an infinite width, and can be described by an array of $T=[t_1, t_2, \ldots, t_m]$, where t_h denotes the thickness of the hth layer from the bottom up. All the dielectric optical thicknesses are limited at the subwavelength range in the visible and near infrared region.

The characteristic matrix method is used to generate training instances [25,26], where we calculate the optical response spectrum for a graphene/Si_3N_4 multilayer nanostructure T with the randomly generated thickness for each Si_3N_4 layer. We focus on investigating the optical properties of monolayer graphene from ultraviolet to near-infrared, which can be described by its dispersive optical conductivity in combination

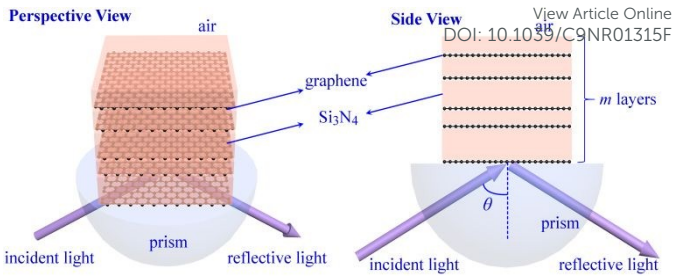

Fig. 1 A multilayer structure composed of m layers of Si_3N_4 and graphene. The excitation light is introduced through a hemispheric prism with an incidence angle θ.

with the Fano model and the Kubo formalism as shown below [26].

$$\sigma_{Fano}(\lambda)=\frac{\sigma_{CB}(\lambda)\cdot(\varepsilon-1)^2}{1+\varepsilon^2}, \qquad \varepsilon=\frac{hc/\lambda-E_r}{\Gamma_r/2} \tag{1}$$

$$\sigma_{Kubo}(\lambda,\mu_c,\Gamma,T)=\sigma_{intra}+\sigma_{inter},$$

$$\sigma_{intra}=\frac{je^2\lambda}{2\pi\hbar^2(\pi c-j\Gamma\lambda)}\int_0^\infty \xi\left(\frac{\partial f_d(\xi,\mu_c,T)}{\partial\xi}-\frac{\partial f_d(-\xi,\mu_c,T)}{\partial\xi}\right)d\xi,$$

$$\sigma_{inter}=-\frac{2je^2(\pi c-j\Gamma\lambda)}{\pi\hbar^2\lambda}\int_0^\infty \frac{f_d(-\xi,\mu_c,T)-f_d(\xi,\mu_c,T)}{4(\pi c-j\Gamma\lambda)^2/\lambda^2-4(\xi/\hbar)^2}d\xi,$$

$$f_d(\xi,\mu_c,T)=\left(e^{(\xi-\mu_c)/k_BT}+1\right)^{-1} \tag{2}$$

In above equations, λ, h and c are the free space wavelength, Plank constant and speed of light in vaccum, respetively; $\hbar$, e and k_B denote the reduced Plank constant, electron charge and Boltzmann constant, respectively; T, ξ and μ_c represent Kelvin temperature, electron energy and chemical potential, respectively; ε is the normalized energy by width Γ_r=0.78eV relative to the resonance energy E_r=5.02eV of the perturbed exciton, and $\sigma_{CB}(\lambda)$ is the continuum background for the Fano model; σ_{intra} and σ_{inter} represent the optical conductivity contributions from the intraband and interband transitions for the Kubo formalism, $f_d(\xi,\mu_c,T)$ is the Fermi-Dirac distribution function, and Γ is scattering rate and is taken as 16.67 ps^{-1} [27]. We take T=300K and μ_c=0.3eV for the next calculation. In the characteristic matrix method, the monolayer graphene layer can be also considered as a lossy dielectric material with a thickness of 0.35 nm and an effective complex refractive index [28], and Si_3N_4 layers and the hemispheric prism are assumed to have the refractive index of 2.0 and 1.46, respectively. The characteristic matrix for the hth layer is represented as below,

$$M_h=\begin{bmatrix}\cos\delta_h & (j/\eta_h)\sin\delta_h\\ j\eta_h\sin\delta_h & \cos\delta_h\end{bmatrix} \tag{3}$$

where $\delta_h=2\pi N_h d_h\cos\theta_h/\lambda$ is the phase factor of the positive-going light wave in the hth layer, and η_h, N_h, d_h and θ_h represent the tilted optical admittance, complex refractive index, thickness and light angle in the hth layer, respectively. The optical response can be calculated through the optical

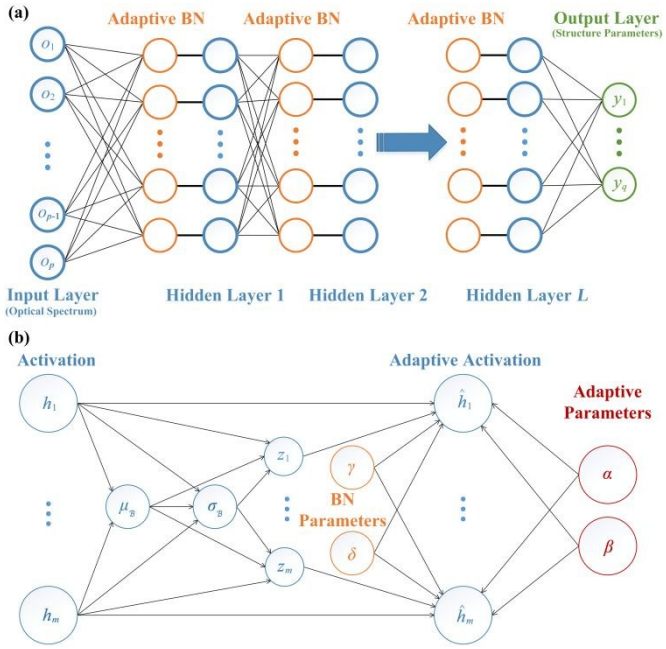

Fig. 2 (a) Architecture of the neural network, where the input is the optical spectrum and the ouput is the structral parameters. (b) Flowchart of an adaptive BN layer, where the output combines activatioin from the previous layer and the BN transformation.

admittance $Y=C/B$ for the assembly from the first layer to the air, which is the ratio of the total tangential magnetic and electric fields as shown below,

$$\begin{bmatrix} B \\ C \end{bmatrix} = M_1 M_2 \ldots M_{h-1} M_h \begin{bmatrix} 1 \\ \eta_a \end{bmatrix} \quad (4)$$

Therefore, the optical response (including the reflectance, transmittance and absorbance) can be expressed as below,

$$R = \left(\frac{\eta_0 B - C}{\eta_0 B + C}\right)\left(\frac{\eta_0 B - C}{\eta_0 B + C}\right)^* \quad (5)$$

$$T = \frac{4\eta_0 \mathrm{Re}(\eta_a)}{(\eta_0 B + C)(\eta_0 B + C)^*} \quad (6)$$

$$A = \frac{4\eta_0 \mathrm{Re}(BC^* - \eta_a)}{(\eta_0 B + C)(\eta_0 B + C)^*} \quad (7)$$

where η_0 and η_a denote the optical admittance of the hemispheric prism and the air, respectively. The number of instances of the optical response typically ranges from thousands to hundreds of thousands.

In view of a standard deep neural network for this inverse problem, we define the training data $D=\{(O_i,Y_i), i = 1,2,\cdots,M\}$, where each O_i and Yi represents a specific optical spectrum and the thickness parameters of the multilayer structure. The neural network is described by a function $f(O_i,Y_i;\Theta)$ parameterized by Θ, which is expected to fit the training data well and have good generalization for the test data. As shown in Fig. 2(a), the network contains an input layer, a series of hiden layers (typically four to seven hidden layers for this case) and an output layer. In the network, L denotes the total number of hidden layers; for the lth hiden layer, $l \in \{1,2,\cdots,L\}$ and N_l is the number of neurons in this layer. The transformation between adjacent layers includes a linear mapping $Z^l = (W^l)^T H^{l-1} + B^l$ with the weight parameter $W^l \in R^{N_l \times N_{l-1}}$ and the bias parameter $B^l \in R^{N_l}$, followed by a neuron-wise nonlinearity activation function $H^l = \emptyset(Z^l)$ [29].The algorithm of stochastic gradient descent is adopted to train the neural network [30]. Particularly, unlike the conventional artificial neural networks, the adaptive batch normalization layers are introduced in addition to the classical multilayer perceptrons, as shown in Fig. 2(a). In front of each hidden layer, there is a layer using the algorithm of adaptive BN, which takes advantage of the state-of-the-art toolkit BN for training the deep network and overcomes the limitation of BN in a small sampling space by an adaptive operation, as shown in Fig. 2(b) and Alg. 1.

Input: Activation h_i for each neuron in a minibatch $\mathcal{B}$ (The number of neruons in $\mathcal{B}$ is m_b); batch normalization parameters γ,δ; adaptive parameters α,β
Output: New activation $\hat{h}_i$ for each neuron;

$\mu_{\mathcal{B}} = \frac{1}{m_b}\sum_{i=1}^{m_b} h_i$ // mean

$\sigma_{\mathcal{B}} = \sqrt{\frac{1}{m_b}\sum_{i=1}^{m_b}(h_i - \mu_{\mathcal{B}})^2}$ // variance

$h_i \leftarrow \alpha h_i + \beta(\gamma y_i + \delta)$ // adaptive activation

Alg. 1 Adaptive batch normalization algorithm

In the algorithm of adaptive BN, γ and δ are parameters of batch normalization, and α and β are adaptive parameters learned from back propagation [31,32]. This algorithm can be assumed as an adpative combination of the standard batch normalization and identity mapping. To reduce the total error at the output layer, the back propagation algorithm would automatically acquire the gradient of α and β. In the training process, α and β play critical roles for the self-adaptation, a bigger value of β means that BN provides more contributions to reduce the error, and a bigger value of α implies that identity mapping provides more contributions. The detailed algorithm for adaptive BN is shown in Alg. 1.

Results and discussion

The purpose of training the artificial neural network is to construct the graphene-based photonic metamaterial corresponding to the on-demand optical response spectrum. Initially, we adpot 50000 spectral training samples for each incident angle, which are calculated by the characteristic matrix method for the specific layer thicknesses. Each sample represents the optical spectrum with 256 step points from o_1 to o_{256} in the wavelength range from 240 nm to 2000 nm. 10 layer thicknesses from y_1 to y_{10} are investigated for the multilayer nanostructure. 1000 additonal samples are generated as the testing set, and they have random thicknesses, which are different from the training set. In order to characterize the performance of the networks, we define the relative spectral error on the testing sets as shown below,

View Article Online
DOI: 10.1039/C9NR01715F

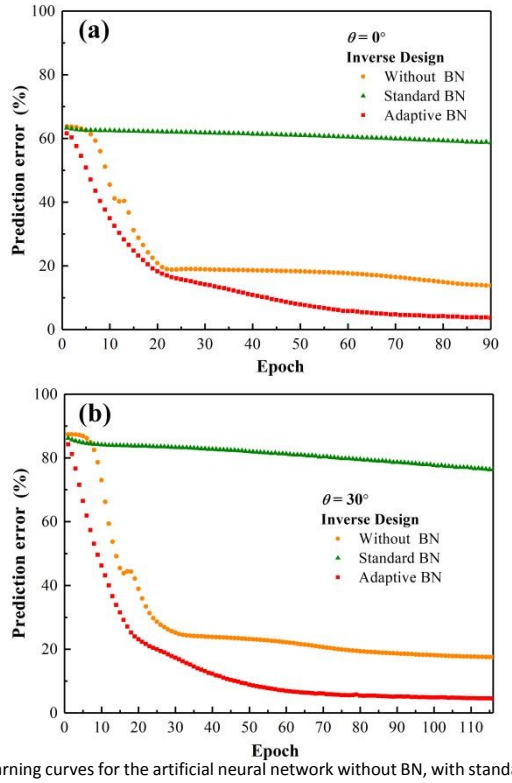

Fig. 3 Learning curves for the artificial neural network without BN, with standard BN and with adaptive BN, respectively. (a) θ=0°. (b) θ=30°. The prediction error at each epoch is the average for 1000 testing samples.

$$\text{Relative Spectral Error} = \frac{\sqrt{\sum_{i=1}^{n}(o_i - p_i)^2}}{\sqrt{\sum_{i=1}^{n} o_i^2}} \quad (8)$$

where o_i is the discretized value for the target spectrum and p_i is the corresponding spectral value predicted. For each sample in the tesing set, Equation (8) evaluates the error between the prediction of the neural network and the authentic spectrum from the characteristic matrix method. The total predition error is the average of error in each testing samples. We use Equation (8) to compare the trained models and the predicting results from three different algorithms.

As shown in Fig. 3(a) and Fig. 3(b), the prediction error barely drops after 90 and 110 epochs for the trainings at θ=0° and θ=30°, respectivley. These results demonstrate that the prediction error for the neural network with standard BN barely drops, indicating its poor performance in designing the thin film structure for the input optical spectrum. Both the neural networks without BN and with adaptive BN have very rapid decreasing of prediction error for test instances, but the error criterions are much higher for the conventional neural network without BN. It is worth mentioning that the method with adaptive BN can reach a very low prediction error (less than 5%) within 100 epochs, which implies very good performance in the optical inverse design for 2D materials.

In order to further demonstrate the advantages of the proposed method, we compare the example test results for the inverse design by using the artificial neural network without BN, with standard BN and with adaptive BN, respectively. As shown in Fig. 4, the networks with the stantard BN for various incident angles bring about significant deviations of spectra (for both transmittance and absorbance) on the predicted nanostructures, which lead to ineffective inverse design and much worse prediction results compared with the conventional

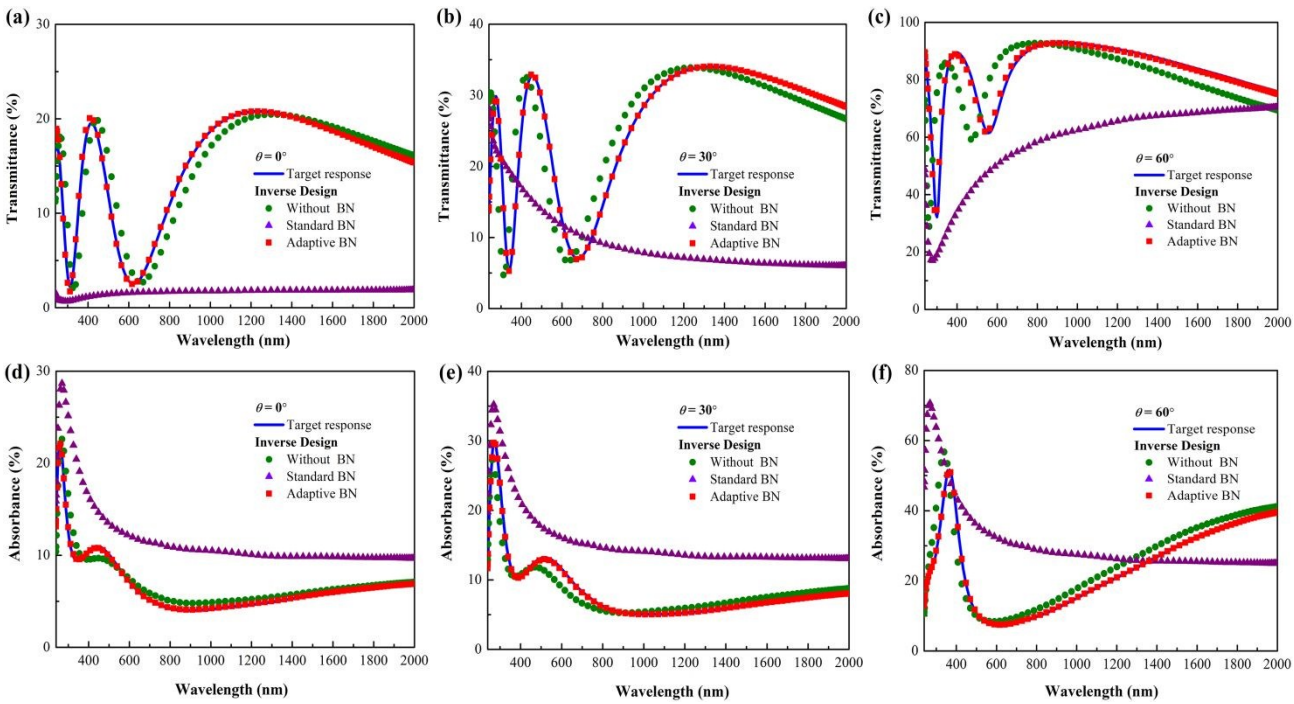

Fig. 4 Example test results for the inverse design by using the artificial neural network without BN, with standard BN and with adaptive BN, respectively. Target optical responses for various incident angles under s-polarized light excitation: (a)-(c) transmittance spectra and (d)-(f) absorbance spectra. The target responses are obtained by the characteristic matrix method with the precise geometry of the metamaterial structures.

View Article Online
DOI: 10.1039/C9NR01315F

Tab. 1 Prediction error of 6 testing samples

Spectral type	Incident angle	Without BN	Standard BN	Adaptive BN
Transmittance	0	14.7%	90.2%	3.2%
	30	19.6%	72.4%	0.9%
	60	14.7%	35.5%	2.2%
Absorbance	0	14.1%	62%	1.4%
	30	13.6%	64.3%	1.1%
	60	15.4%	70.7%	0.7%

artificial neural network without BN. The predicted transmittance in Fig. 4(a) is even totally incorrect for the case of normal incidence. The serious prediction errors could be attributed to the small sampling space with an inadequate batch stastics estimation. In contrast, when the adaptive parameters α and β for BN are introduced, the effectiveness and accuracy of inverse design are dramatically improved for both transmittance and absorbance spectra at various incident angles, as shown in Fig. 4. There are 6 testing samples in Fig. 4 with different types of spectra and incident angles. Tab. 1 lists the relative spectral error of these samples by comparing the use of three methods. As shown in Tab. 1, the use of adaptive BN demonstrates much more precise prediction with the maximum deviation less than 3.2% versus the artificial neural networks without BN and with standard BN.

Finally, we demonstrate two examples of designing metamaterials with graphene to achieve the goals of low absorbance and near-unity absorbance for a specific incidence angle from ultra-violet to near-infrared, as shown in Fig. 5. It is worth mentioning, the optical responses in our work are mainly obtained by the characteristic matrix method, which is a precise and efficient approach for getting spectral samples, and they can be generated by other computational methods. We plot the target absorbance ratios by both the characteristic matrix method and the finite element method as a comparison. These results demonstrate Fig. 5(a) indicates the target spectrum with a low absorbance ratio at normal incidence, which has the peak absorbance of only about 18% around the wavelength of 307 nm and possesses the absorbance no more than 8% for the wavelengths from 500 nm to 2000nm. The predicted thickness parameters are 0.35 nm/2.8 nm/0.35 nm/13.6 nm/0.35 nm/28.6 nm/0.35 nm/33.8 nm/0.35 nm/14.5 nm. The designed nanostructure shows very good consistency on the absorbance spectrum with the target spectrum obtained by the characteristic matrix method. Fig. 5 (b) shows a structure whose target is near-unity optical absorbance in graphene at a central wavelength of 1268 nm by using the incident angle of 85°. The thickness parameters of this 10-layer nanostructure are 0.35 nm/19.5 nm/0.35 nm/19.5 nm/0.35 nm/19.0 nm/0.35 nm/19.2 nm/0.35nm/20.3 nm. The designed nanostructure also demonstrates high accuracy on the absorbance consistency with the target spectrum obtained by the characteristic matrix method. These two examples further illuminate the solid effectiveness and high accuracy of adaptive BN in artificial neural network for the inverse optical design based on 2D materials. Our method has been developed as an open-source Python programming package for the deep-learning study and inverse design of nanoscale optics based on graphene and other 2D materials (See the supplementary information). The latest package coding information can be also accessed by the website https://github.com/closest-git/MetaLab. This tool kit will dramatically facilitate the optical engineering and application of 2D materials and related devices.

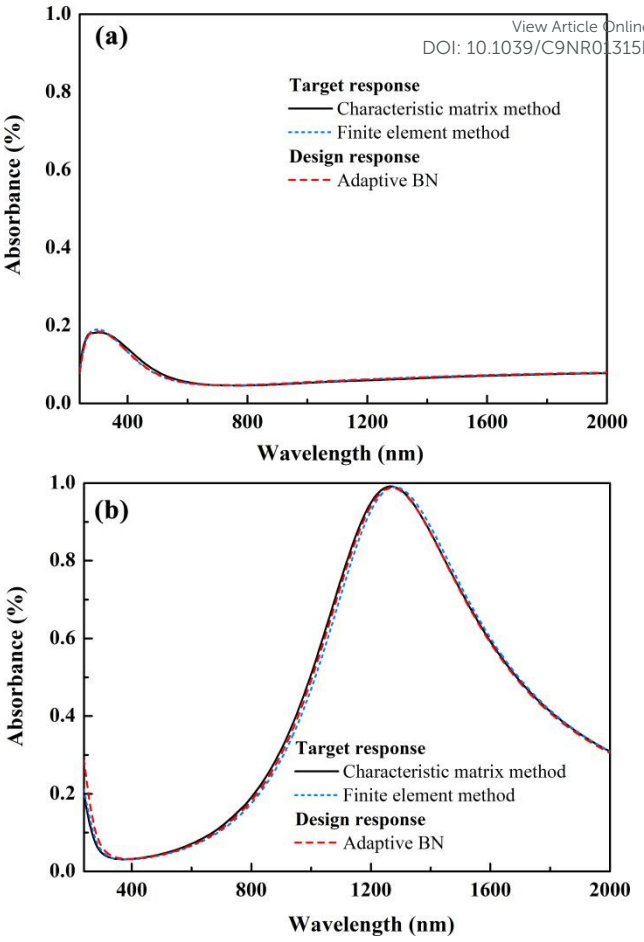

Fig. 5 Optical response for designed nanostructures under *s*-polarized light excitation. (a) Low absorbance in graphene. (b) Near-unity absorbance in graphene.

Conclusions

We introduce adaptive batch normalization in the artificial neural network for the inverse optical design of photonic metamaterials with 2D materials. Our method demonstrates extremely high accuracy for the spectral prediction of multilayer nanostructures with graphene monolayers. The approach also effectively addresses the currently inaccessible inverse problem of designing a geometry for a desired optical response spectrum and also significantly speeds up the direct spectrum prediction of such sub-wavelength structures. This approach breaks the ground for the on-demand design of optical response for nanophotonics applications, and can be extended to many other advanced optical devices based on 2D materials.

Conflicts of interest

There are no conflicts to declare.

Acknowledgements

This work was supported by NSAF (Grant No. U1830116), Shenzhen Science and Technology Innovation Commision (JCYJ20170306141755150), Natural Science Foundation of Guangdong Province (2018A030313299), Fujian Provincial Department of Science and Technology (2017J01123), China Scholarship Council, and National Natural Science Foundation of China (61307042).

Notes and references

‡ Footnotes relating to the main text should appear here. These might include comments relevant to but not central to the matter under discussion, limited experimental and spectral data, and crystallographic data.

1 K. S. Novoselov, A. Mishchenko, A. Carvalho and A. H. C. Neto, *Science,* 2016, **353**, aac9439.
2 Y. Li and T. F. Heinz, *2D Mater,* 2018, **5**, 025021.
3 F. Xia, H. Wang, D. Xiao, M. Dubey and A. Ramasubramaniam, *Nat. Photon.,* 2014, **8**, 899-907.
4 Y. Fan, N-H. Shen, F. Zhang, Q. Zhao, H. Wu, Q. Fu, Z. Wei, H. Li and C. M. Soukoulis, *Adv. Opt. Mater*, 2018, 1800537.
5 Y. Cai, J. Zhu, Q.H. Liu, T. Lin, J. Zhou, L. Ye, Z. Cai, *Opt. Express,* 2015, **23**, 32318-32328.
6 Y. Cai, J. Zhu and Q.H. Liu, App. Phys. Lett., 2015, **106**, 043105.
7 K. F. Mak and J. Shan, *Nat. Photon.*, 2016, **10**, 216-226.
8 J. Zhu, Q. H. Liu, T. Lin, *Nanoscale*, 2013, **5**, 7785-7789.
9 J. Zhu, S. Yan, N. Feng, L. Ye, J.Y. Ou and Q. H. Liu *Appl. Phys. Lett.,* 2018, **112**, 153106.
10 I. S. Nefedov, C. A. Valagiannopoulos and L. A. Melnikov, *J. Optics,* 2013, **15,** 114003.
11 Y.C. Chang, C.H. Liu, C.H. Liu, S. Zhang, S. R. Marder, E. E. Narimanov, Z. Zhong and T. B. Norris, *Nat. Commun.,*2016, **7**, 10568.
12 X.L. Li, W.P. Han, J.B. Wu, X.F. Qiao, J. Zhang and P.H. Tan, *Adv. Funct. Mater.,* 2017, **27**, 1604468.
13 Z. Yu, H. Cui and X. Sun, *Opt. Lett.,* 2017, **42**, 3093-3096.
14 J. C. C. Mak, C. Sideris, J. Jeong, A. Hajimiri and J. K. Poon *Opt. Lett.,* 2016, **41**, 3868-3871.
15 Piggott A Y, Lu J, Lagoudakis K G, Petykiewicz J, Babinec T M, and Vučković J 2015 Nat. Photonics 9 374-377.
16 L. F. Frellsen, Y. Ding, O. Sigmund and L. H. Frandsen, Opt. Express, 2016, **24**, 16866-1683.
17 W. Zhang and Liu Q. H. IEEE T. Geosci. Remote., 2015, **53**, 429-439.
18 Z. Jin, S. Mei, S. Chen, Y. Li, C. Zhang, Y. He, X. Yu, C. Yu, J. K. W. Yang, B. Luk'yanchuk, S. Xiao and C.-W. Qiu, ACS Nano, 2019, **13**, 821-829.
19 J. Peurifoy, Y. Shen, L. Jing, Y. Yang, F. Cano-Renteria, B. G. DeLacy, J. D. Joannopoulos, M. Tegmark and M. Soljačić, Sci. Adv., 2018, **4**, eaar4206.
20 D. Liu, Y. Tan, E. Khoram and Z. Yu, ACS Photonics, 2018, **5**, 1365-1369.
21 W. Ma, F. Cheng and Y. Liu, ACS Nano, 2018, **12**, 6326-6334.
22 S. Inampudi and H. Mosallaei, Appl. Phys. Lett., 2018, **112** 241102.
23 M. Itzik, M. Mrejen, A. Nagler, U. Arieli, L. Wolf and H. Suchowskii Light-Sci. Appl., 2018, **7**, 60.
24 S. Ioffe and C. Szegedy, Proc. Int. Conf. Mach. Learn., 2015, 448-456.
25 H. A. Macleod, Thin-Film Optical Filters, CRC Press, Florida, 2010.
26 J. Zhu, C. Li, J.-Y. Ou and Q. H. Liu, Carbon, 2019, **142**, 430-437.
27 Q. Zhang, X. Li, M. M. Hossain, Y. Xue, J. Zhang, J. Song, J. Liu, M. D. Turner, S. Fan, Q. Bao and M. Gu, Sci. Rep. 2014, **4**, 6559.
28 J. Zhu, J. Cheng, L. Zhang and Q. H. Liu, Mater. Lett., 2017, **186**, 53-56.
29 C. M. Bishop, Neural Networks for Pattern Recognition, Clarendon Press, Oxford, 1995.
30 L. Bottou, Proc. COMPSTAT 177-186, 2010.
31 D. E. Rumelhart, G. E. Hinton and R. J. Williams, Nature, 1986, **323**, 533.
32 A. Géron, Hands-on Machine Learning with Scikit-Learn and TensorFlow: Concepts, Tools, and Techniques to Build Intelligent Systems, O'Reilly Media, Inc, Sebastopol, 2017.

View Article Online
DOI: 10.1039/C9NR01315F